A MODEL FOR ASSESSING THE RISK OF LIQUID HYDROGEN TRANSPORT THROUGH ROAD TUNNELS

Caliendo, C.[1], Genovese, G.[2,3], Markert, F.[3] and Russo, P.[4]

[1] Department of Civil Engineering, University of Salerno, Via Giovanni Paolo II, 132-84084 Fisciano, Salerno, Italy, ccaliendo@unisa.it
[2] Department of Civil Engineering, University of Salerno, Via Giovanni Paolo II, 132-84084 Fisciano, Salerno, Italy, ggenovese@unisa.it
[3] DTU Civil and Mechanical Engineering, Technical University of Denmark, Brovej 118, Kongens, Lyngby, 2800, Denmark, fram@byg.dtu.dk
[4] Department of Chemical Engineering Materials Environment, Sapienza University of Rome, Via Eudossiana 18, 00184, Rome, Italy, paola.russo@uniroma1.it

ABSTRACT

Among the new energy carriers aimed at reducing greenhouse gas emissions, the use of hydrogen is expected to grow significantly in various applications and sectors (i.e., industrial, commercial, transportation, etc.) due to its high energy content by weight and zero carbon emissions. The increasingly widespread use of hydrogen will require massive distribution from production sites to final consumers, and the delivery by means of liquid hydrogen road tankers may be a suitable cost-effective option for market penetration in the short-medium term. Liquid hydrogen (LH_2) presents different hazards compared to gaseous hydrogen, and an accidental release in confined spaces, such as road tunnels, might lead to the formation of a flammable hydrogen cloud that might deflagrate or even detonate. Nevertheless, the potential negative effects on users in the event of accidental leakage of liquid hydrogen from a tanker in road tunnels so far have not been sufficiently investigated. Therefore, a 3D Computational Fluid Dynamics model for the release of LH_2 and its dispersion within a road tunnel was developed in this study. The proposed model was validated by a comparison with certain experimental and numerical studies found in the literature. Such modeling is demanding for long tunnels. Therefore, the results of the simulations (e.g., the amount of hydrogen contained within the cloud) were combined with established simplified consequence methods to estimate the overpressures generated from a potential hydrogen deflagration. This was then used to evaluate the effects on users while evacuating from the tunnel. The findings showed that the worst scenario is when the release is in the middle of the tunnel length and the ignition occurs 90 s after the leakage.

Keywords: Liquid hydrogen release; Road tunnels; Computational fluid dynamics; Risk assessment.

NOMENCLATURE

Symbol	Parameter	Unit
ρ_{H2}	Liquid density of hydrogen	kg/m^3
A	Area of the hole	m^2
C_D	Discharge coefficient	-
$\dot{m}$	Mass flow rate	kg/s
P_{tank}	Tank pressure	Pa
P_{atm}	Atmospheric pressure	Pa
g	Gravity acceleration	m/s^2
h	Height of liquid above the hole	m
m_{TNT}	Equivalent mass of TNT	kg
α	Equivalency factor	-
m_{H2}	Mass of hydrogen	kg
H_{H2}	Heat of combustion of hydrogen	J/kg
H_{TNT}	Heat of combustion of TNT	J/kg

1.0 INTRODUCTION

One of the Green Deal's objectives is to reduce greenhouse gas emissions by at least 50% by 2030 compared to the '90s, with the goal of achieving climate neutrality in Europe by 2050 [1]. Because of its zero carbon emissions and high energy content by weight, hydrogen has the potential to help mitigate the current rapid climate change and achieve the goals of this agreement if used in various applications and sectors (i.e., industrial, commercial, transportation, etc.). The growing use of hydrogen as an energy carrier will, however, necessitate massive distribution from production sites to final consumers, thus cost-effective methods of storing and transporting hydrogen must be taken into consideration. Hydrogen can be transported via road, rail, water, and pipelines; intermodal transportation, which considers multiple modes at the same time, might also be a suitable approach [2]. However, hydrogen needs to be compressed or liquified due to its very low density at ambient conditions. In this respect, transport volumes and delivery distances determine the competitiveness of each mode of transportation and storage [3]. Transportation by pipeline might be the best and safest method but only in the long run since the development of an extensive hydrogen pipeline network will require considerable investment due to both the choice of materials that should be able to withstand higher pressures than the existing natural gas pipelines and operational safety issues [4]. In the short-term perspective, instead, delivery by road transport might represent the optimal solution. Specifically, compressed gaseous hydrogen tube trailers might be appropriate for transportation over short distances; while storage in liquid form is the most suitable choice over longer distances [5], [6]. Although liquid hydrogen (LH$_2$) road trucks have higher operating costs because of the liquefaction of hydrogen, they can carry much more hydrogen than compressed hydrogen tube trailers, which makes them the most cost-effective option for market penetration in the short-medium term [7]. However, LH$_2$, which is typically stored at extremely low temperatures within super-insulated cryogenic tankers, presents different hazards and risks compared to those related to the more commonly known compressed gaseous hydrogen [8]. An accidental release of large quantities of LH$_2$ might lead to the formation of a flammable hydrogen-air mixture that might deflagrate or even detonate. This represents a safety issue that must be addressed to reduce the risk to the public [9], [10]. In fact, the flammable cloud might be significantly larger than that induced by a gaseous hydrogen release due to the high density and vaporization, which also increases the intensity and distance of the adverse effects if ignited [11]. In this respect, the consequences of a LH$_2$ leakage might be much more severe if it occurs in a confined space, such as a road tunnel, since the hydrogen mixture can be trapped by the tunnel ceiling increasing the risk of explosion [12]. This might result in catastrophic property damage as well as fatalities [13], [14]. In such context, the accurate analysis of the development of the flammable hydrogen cloud in the event of an accidental leakage is critical for determining the risk due to vehicles transporting LH$_2$, especially through road tunnels [10].

Over the last few years, many studies have investigated the consequences of LH$_2$ release both experimentally and by means of numerical modeling. Statharas et al. [15], using a 3D Computational Fluid Dynamics (CFD) code, modeled the experiments of LH$_2$ dispersion in the open and in presence of buildings to describe the complex behavior of cold hydrogen spills. Sklavounos and Rigas [16] numerically investigated the behavior of cryogenic hydrogen releases in the open. Middha and Hansen [17] simulated the release of both liquid and compressed hydrogen from hydrogen-fuelled vehicles in two different tunnel layouts and longitudinal ventilation conditions. Several experimental tests on LH$_2$ spills in the open environment were carried out by the Health and Safety Laboratory (HSL) [6] to identify the main issues concerning hydrogen transport and storage. The diffusion behavior of LH$_2$ spills on different surfaces, such as gravel, concrete, or steel, has also been investigated by Unno et al. [18]. Jin et al. [19] investigated the effects of the ground temperature and wind velocity on LH$_2$ dispersion in open space; while Liu et al. [20] focused on the impact of the source condition (i.e., the mass flow rate and spill amount). Giannissi and Venetsanos [21] carried out CFD simulations to explore the effect of ambient humidity on cryogenic hydrogen spills. Liu et al. [22] compared the spread of the flammable vapor cloud in the event of LH$_2$ spills in open air. Pu et al. [23] conducted a numerical study on the dispersion behavior and hazard identification of LH$_2$ release in an unconfined area to investigate the probability of fire and/or explosion. Hansen [24] compared the hazard distances resulting from LH$_2$ and LNG (Liquefied Natural Gas) in the presence of wind in an open environment. Tang et al. [24], based on CFD simulations, investigated the dispersion behavior of an amount of LH$_2$

release in a short tunnel in the presence of natural ventilation. Ustolin and Paltrinieri [26], using different empirical correlations, estimated the dimension and duration of a LH_2 fireball after the catastrophic rupture of a tank in an open environment. Caliendo and Genovese [27], by means of an approximate method, carried out a preliminary study concerning the quantitative risk assessment on the transport of dangerous goods through road tunnels, including LH_2. Liu et al. [28], through a CFD software, predicted the safe distance of LH_2 spills in an open environment as a function of the spill rate and wind speed. Finally, the former PRESLHY project [29], aimed at increasing the knowledge for a safer use of LH_2, focused on many safety aspects relating to dispersion, ignition, and combustion (i.e., the burning process of hydrogen with oxygen), by also providing some engineering correlations to assess the consequences of LH_2 release mostly in the open atmosphere; while the new ELVHYS project aimed at improving safety and efficiency of liquid hydrogen transfer technologies.

The above chronological literature review shows that most of the studies have prevalently focused on the consequences of LH_2 releases in open spaces, but very few authors have dealt with their effects in confined spaces as tunnels. Specifically, the potential negative effects on users in the event of an accidental release of large quantities of LH_2 from a tanker in a road tunnel so far appear not to have been sufficiently investigated. This represents a lack of knowledge that this paper will attempt to fill.

2.0 ROAD TUNNEL DESCRIPTION

2.1 Geometric and functional characteristics

In this study, we have investigated an existing Italian twin-tube motorway tunnel with each tube normally used for traffic in one driving direction, and a length of 1 km. The cross-section of each tube has a typical horseshoe shape. It has a total width of 10.5 m (i.e., two lanes of 3.75 m, two sidewalks of 1 m, and two shoulders of 0.5 m that separate the driving lane from the sidewalks), and a maximum height of 7 m. The tunnel is assumed to be straight, flat, and with an emergency exit located in the middle of the tunnel length (i.e., 500 m from the entrance portal). The tunnel is designed in compliance with the minimum safety requirements of Directive 2004/54/EC [30], according to which a mechanical ventilation system is not mandatory for road tunnels with lengths ≤ 1 km, as it is in our case. Therefore, only the natural ventilation due to the piston effect of vehicles in motion is considered. To take this into account a positive pressure difference of 5 Pa [31] between the entrance and the exit portal of each tunnel tube was assumed. The walls of each tunnel tube and ceiling have a thickness of 0.5 m and they are made of concrete (i.e., density of 2585 kg/m^3, thermal conductivity of 1.67 W/m/K, and specific heat of 0.94 kJ/kg/K taken from literature [32]); whereas the road pavement was modeled as asphalt mixture with a thickness of 0.4 m, the density of 2275 kg/m^3, the thermal conductivity of 0.56 W/m/K, and specific heat of 0.88 kJ/kg/K [33]. Figure 1 shows the twin-tube motorway tunnel, as well as the cross-section of the investigated tube in which an accident scenario, with the associated release of LH_2, was assumed to occur.
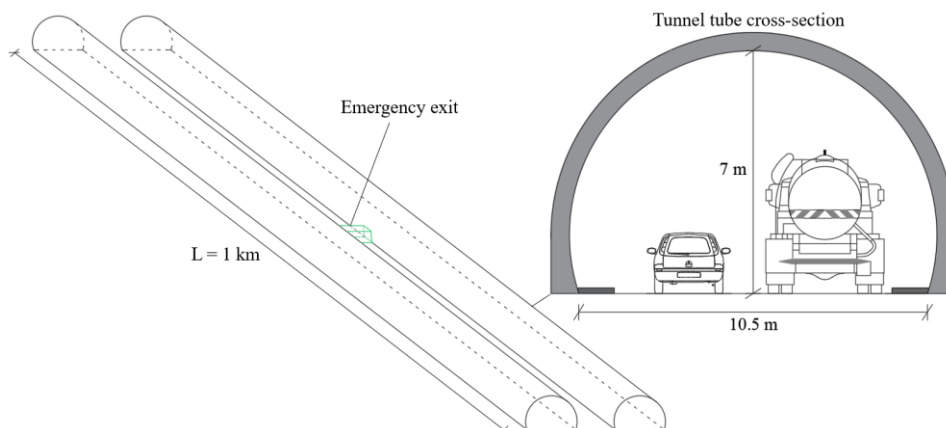
Figure 1. Twin-tube motorway tunnel, as well as the cross-section of the investigated tube in which an accidental release of LH_2 is assumed to occur.

2.2 Traffic

The traffic flow considered in this study was expressed in terms of Peak Hour of traffic Volume

(PHV), which was computed to be about 1243 vehicles/hour per lane, with a percentage of Heavy Goods Vehicles (HGVs) of 25% (including 2% of buses) [34].

2.3 Accidental release scenarios

Five different positions (i.e., 165, 335, 500, 670, and 835 m from the entrance portal of the tube), were considered for the road tanker to stop in the tube after an accidental event and to start the release of LH$_2$ from a hole. In this respect, it is to be said that LH$_2$ for road transport is typically assumed to be stored in 45 m^3 super-insulated tankers, which can contain up to 2.5·10^3 kg of LH$_2$ considering an 80% state of charge, at about 400,000 Pa pressure and 20 K [35]. The release was considered to be the consequence of a traffic accident that generates a hole at the bottom rear side of the road tanker (i.e., 50 cm above the road pavement), the diameter of which was assumed to be 50 mm. The resulting LH$_2$ mass flow rate from the hole was computed according to [36]:

$$\dot{m} = \rho_{H2}AC_D\sqrt{\frac{2(P_{tank}-P_{atm})}{\rho_{H2}} + 2gh} \,, \tag{1}$$

where $\dot{m}$ – mass flow rate, kg/s; ρ_{H2} – liquid density of hydrogen, kg/m^3; A – area of the hole, m^2; C_D – discharge coefficient; P_{tank} – tank pressure, Pa; P_{atm} – atmospheric pressure, Pa; g – gravity acceleration, m/s^2; h – height of liquid above the hole, m. Given that ρ_{H2} is 70.8 kg/m^3, A is 1.93·10^{-3} m^2, C_D is 0.6 according to [37], P_{tank} is 400,000 Pa, P_{atm} is 101,325 Pa, g is 9.81 m/s^2, and h is 2 m, by applying Eq. (1), the obtained mass flow rate is 7.68 kg/s. This means that the LH$_2$ release from the tanker lasts approximately 5.4 min.

2.4 Schematization of queued vehicles and people evacuation process

The vehicles in the queue upstream of the release were schematized as parallelepipeds with dimensions of 6 m (length) × 1.8 m (width) × 1.5 m (height) and were modeled assuming that: (i) they stop without passing the LH$_2$ road tanker; (ii) the safety distance between each vehicle in the queue is 2 m; (iii) the first queued vehicle is at a distance of 10 m from the rear side of the LH$_2$ road tanker; (iv) vehicles downstream of the accident leave the tunnel tube from the exit portal without any issues. Based on these assumptions, the number of vehicles upstream of the release is 18, 39, 60, 81, and 102 per lane, when the LH$_2$ road tanker, after the incident, stops at 165, 335, 500, 670, and 835 m from the entrance portal of the tunnel tube, respectively. Considering that the average occupancy rate is about 2 people per vehicle (i.e., 1.7 people for cars [38], 1 for HGVs, and 30 for buses), the total number of people evacuating from the tube was computed to be 72, 156, 240, 324, and 408 when the release of LH$_2$ occurs at the respective stops described above. Users are assumed to escape through the entrance portal of the tube when the tanker stops upstream or in proximity of the emergency exit located in the middle of the tunnel length; while if it occurs downstream of the emergency exit users are considered to escape partly through the emergency exit and partly through the entrance portal. The users' pre-movement time, which includes the detection and reaction time, was assumed to be equal to 90 s, while the walking speed was equal to 0.5 m/s. Figure 2 shows a schematic layout of the vehicles in the queue upstream of the LH$_2$ road tanker for the tunnel tube investigated.

Figure 2. Layout of the vehicles in the queue upstream of the LH$_2$ road tanker for the tunnel tube investigated.

3.0 NUMERICAL MODELING

3.1 Brief description of the simulation code

The simulations were carried out using ANSYS Fluent, version 2022 R1 [39], widely applied for simulating LH$_2$ release and dispersion phenomena both in the open atmosphere and confined spaces [20], [22], [23], [25], [28], [40], [41]. The transient two-phase flow consisting of LH$_2$ release and the subsequent formation of the vapor cloud was simulated by the mixture model [39], [40]. Specifically,

4

the liquid phase includes liquid hydrogen, while the gas phase consists of the hydrogen-air mixture and all the gases are assumed to be incompressible due to the Mach number of the flow in the domain less than 1.0 (for more details about the boundary conditions see Section 3.3). In the mixture model, the mass transfer from the liquid phase to the gas phase and vice versa is governed by the evaporation-condensation Lee model in which the saturation temperature was set equal to 20.27 K [42]. For the turbulence closure, the k-ε model was chosen as the most appropriate closure when dealing with heavy gas dispersion in the presence of obstacles [41], as well as to account for any buoyancy effect [43]. To improve the efficiency of calculation, the Pressure-Implicit with Splitting of Operators (PISO) algorithm for pressure-velocity coupling, was adopted. The solution convergence is considered to be achieved when the residual is below 10^{-3}; whereas the time step of the simulations was set to 10^{-3} s as also selected in other studies [20], [23], [25], [40]. It is to be stressed that a time step dependence analysis was also carried out (but not reported) finding that 10^{-3} s is a good compromise between the accuracy of the results and the computational time. The main input data to be defined to simulate the LH_2 release are the tunnel geometry, location and dimension of the tanker and the release source, the mass flow rate from the hole, position and geometry of queued vehicles, and the pressure difference between the entrance and exit portal to account for the natural ventilation.

3.2 Code validation

3.2.1 Comparison with an experimental test of LH_2 release in the open

The LH_2 release model was preliminarily validated against an experimental test performed by NASA [44] consisting of a downward release of 5.7 m^3 LH_2 within approximately 35 s in the open. The scenario was reproduced using ANSYS Fluent and the simulated results were compared with the experimental ones. The domain had dimensions of 200 m (length) × 60 m (width) × 80 m (height), which was subdivided into cells of 1.5 m side locally refined at the domain near the source up to 5 cm [20]. Figure 3 shows a comparison of the contours of hydrogen concentrations between the experimental data by the NASA test and the simulated results using ANSYS Fluent after 20.94 s from the release. From Figure 3 it can be noted that the CFD code is able to accurately reproduce the vapor cloud formation as a consequence of the LH_2 release into the atmosphere. The little discrepancies between the experimental and simulation results might be due to the fluctuation of the wind speed in the actual scenario that was only approximated by constant wind speed and direction in the simulation.
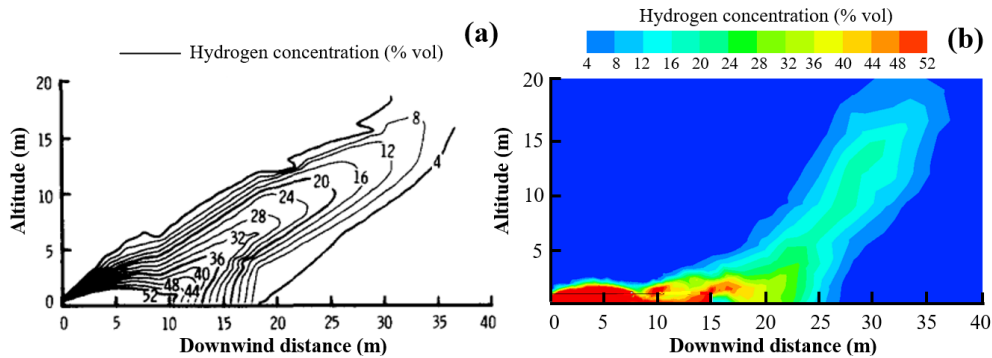
Figure 3. Hydrogen concentration contours after 20.94 s from the release: (a) Experimental results; (b) Simulated results.

3.2.2 Comparison with a numerical study of LH_2 release in a confined space

In order to validate the CFD code also with respect to LH_2 releases in confined spaces, the model developed by Tang et al. [25] was reproduced by using ANSYS Fluent. The model consisted of a LH_2 release through a leakage diameter of 26 mm with a mass flow rate of 1 kg/s for a total of 5.6 s in a 53 m-long naturally ventilated tunnel. The total number of grids was equal to 176,000, which was obtained by using a mesh size of 42 cm side with a local refinement of 1 cm near the release source. The size of the simulated flammable hydrogen cloud (i.e., with a hydrogen concentration range between 4 and 75% by volume in air) over time has been compared with that obtained by the aforementioned numerical study found in the literature. Figure 4 shows the comparison between the simulation results by Tang et al. [25] and those computed in this work: an error of less than 5% was

found, thus proving the ability of the presented author's model to correctly simulate LH_2 release also in confined spaces. In light of the above-mentioned findings (i.e., the ability of the CFD code to correctly reproduce hydrogen cloud formation after liquid release both in open and confined space), we subsequently set up our 3D CFD modeling for the full-scale tunnel tube investigated in this paper.
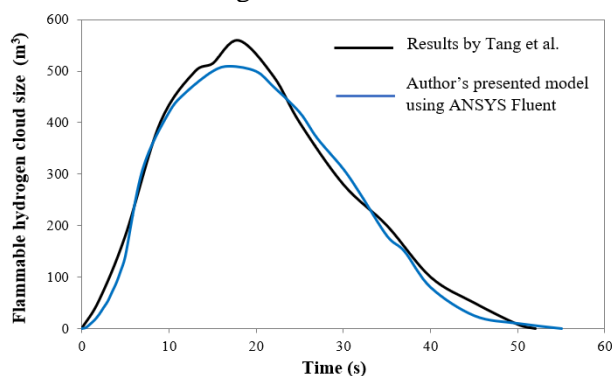
Figure 4. Comparison between the flammable hydrogen cloud size by Tang et al. [25] and the simulated results by the author's presented model using ANSYS Fluent.

3.3 Computational domain and boundary conditions

The 3D computational domain consists of a horseshoe-shaped tunnel tube of 1 km long with a maximum height and width of 7 and 10.5 m, respectively. The LH_2 road tanker − which was assumed to be located in the middle of the right driving lane and 0.5 m above the road pavement − was schematized as a cylinder with a length of 12 m and diameter of 2.2 m for a total volume of about 45 m^3. A tetrahedral mesh of 1 m side was chosen for the computational domain (i.e., the entire tunnel length), whereas a local refinement characterized by cells with a 25 mm side (i.e., half of the diameter of the hole surface) was made around the release region in order to obtain a more accurate evaluation of the hydrogen concentrations. Therefore, the mesh length scale gradually coarsened from 25 mm up to 1 m for each subsequent element away from the release region. The extension of the transition zone between the finest and coarsest mesh was found to cover a distance of about 2 m from the release region. Figure 5 provides a view of the computational mesh with the detail of the mesh refinement around the release region. The LH_2 release was modeled in the simulations by imposing a constant mass flow rate to a surface of 50 mm diameter located at the bottom rear side of the tanker. Atmospheric initial conditions within the tunnel tube were set with pressure 101,325 Pa and temperature 288 K, while a positive pressure difference of 5 Pa was defined between the entrance and exit portal in order to consider the piston effect of moving vehicles. Pressure inlet and pressure outlet boundary conditions were assigned to the entrance and exit portal surfaces, respectively.
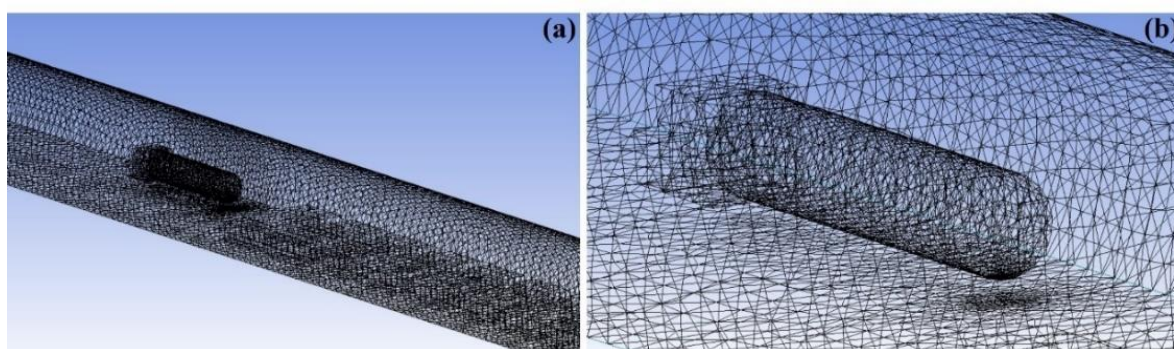
Figure 5. Computational mesh: (a) Tunnel region away from the release; (b) Detail of the mesh refinement around the release region.

3.4 Grid sensitivity analysis of the full-scale tunnel investigated

Given the lack of a literature reference for the model of the tunnel investigated an intrinsic grid sensitivity analysis for the full-scale tunnel was carried out to define the mesh resolution that was a good compromise between the accuracy of the results and the computational time. Different tetrahedral cell sizes for the entire tunnel length ranging from 2 m to 0.5 m side were investigated. As

6

mentioned before, for all the mesh sizes investigated, a local refinement up to 25 mm was made in the vicinity of the release region. Figure 6 shows, for the different mesh sizes investigated, the hydrogen concentration over time simulated in the centre of the right driving lane at a height of 6 m and 10 m upstream of the release when the LH_2 road tanker is in the middle of the tunnel length. This above-mentioned location was chosen because of the high buoyancy of hydrogen, which tends to accumulate under the tunnel ceiling. From Figure 6, it can be noted that using a mesh size smaller than 1 m side did not significantly increase the model accuracy (i.e., the error between the simulation results for a mesh size of 1 m and 0.5 m was less than 5%) but only the computational time. On this basis, the tunnel volume was divided into a total of 454,550 tetrahedral cells having 1 m side far from the leakage source with a minimum size of 25 mm close to the release location. It is to be stressed that the selected mesh size for the investigated road tunnel is in line with the study by Molkov and Dery [45], in which a mesh size of 2-3 cm and 75 cm was used near the source and for the remaining part of the tunnel, respectively.
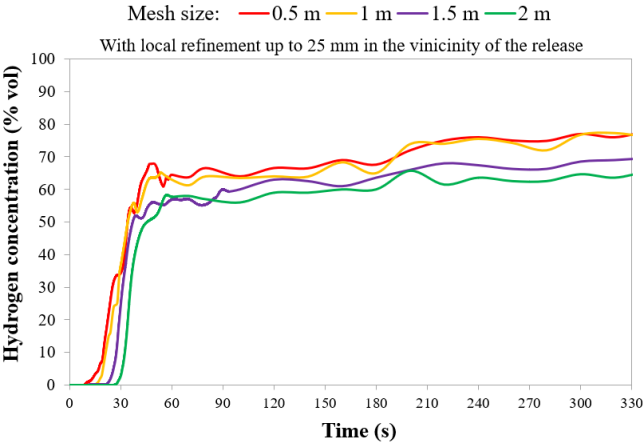
Figure 6. Grid sensitivity analysis: hydrogen concentration at the centre of the right driving lane at a height of 6 m and 10 m upstream of the release location.

4.0 RESULTS

4.1 Hydrogen dispersion

The duration of the release lasts 5.4 min, while the simulations were carried out for a total of 10 min to take into account the people evacuation process from the tunnel. During the release, LH_2 evaporates by exchanging heat with the surrounding environment and it disperses quickly by accumulating under the tunnel ceiling due to the difference in density between air and hydrogen. The propagation of the flammable hydrogen cloud over time within the investigated tunnel tube is depicted in Figure 7. In this respect, the simulation took about 110 h running in a modern 8-core personal computer.
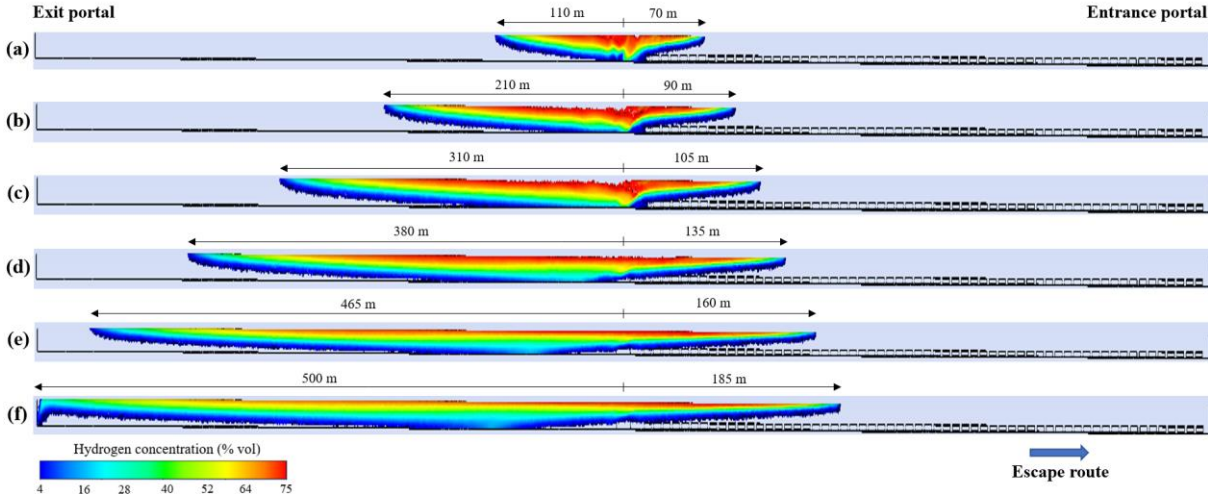
Figure 7. Contours of flammable hydrogen cloud propagation within the investigated tube when the release location is in the middle of the tunnel length after: (a) 100 s; (b) 200 s; (c) 300 s; (d) 400 s; (e) 500 s; (f) 600 s.

It is worth highlighting that hydrogen concentration is well stratified in the vertical direction with higher values located near the ceiling. From Figure 7, it can also be noted that the development of the flammable hydrogen cloud is not symmetrical upstream and downstream of the release location due to the natural ventilation that pushes hydrogen toward the exit portal of the tube. Specifically, the flammable hydrogen cloud reaches a distance of 70, 90, 105, 135, 160, and 185 m upstream of the release location after 100, 200, 300, 400, 500, and 600 s from the start of release.

4.2 Hydrogen deflagration

4.2.1 Generality

Depending on the environmental characteristics (i.e., traffic congestion and/or confinement) and the ignition source, after the LH_2 release, either a deflagration or detonation might occur once the mixture has been ignited. It is to be mentioned that almost all vapor cloud explosions begin as low-speed deflagrations unless a massive ignition source is present [36]. The effects, in terms of overpressures, of a deflagration in a confined space (e.g., a road tunnel) significantly differ from those in the open. In this respect, few studies available in the literature have proposed simplified engineering correlations to estimate the overpressures generated from deflagrations in confined environments. Among them, Liu et al. [46], by means of FEM simulations, developed a model for estimating the blast wave propagation inside tunnels; whereas Silvestrini et al. [47], have provided an analytic method for evaluating blast-wave overpressures in confined geometries starting from open-space blast data. Each method has its own strengths and weaknesses in terms of applicability, however, the method proposed by Silvestrini et al. [47] was found to better reproduce the overpressures over distance simulated by Li [36] for a hydrogen deflagration in a full-scale tunnel, as shown in Figure 8. This is due to its capability to consider the geometry of confinement (i.e., the tunnel cross-section), the mass of fuel involved in the deflagration, and the distance from the ignition location. Therefore, in the present paper, the results of the 3D simulations of the hydrogen dispersion were combined with the Silvestrini's method to estimate the overpressures generated from a potential hydrogen deflagration.
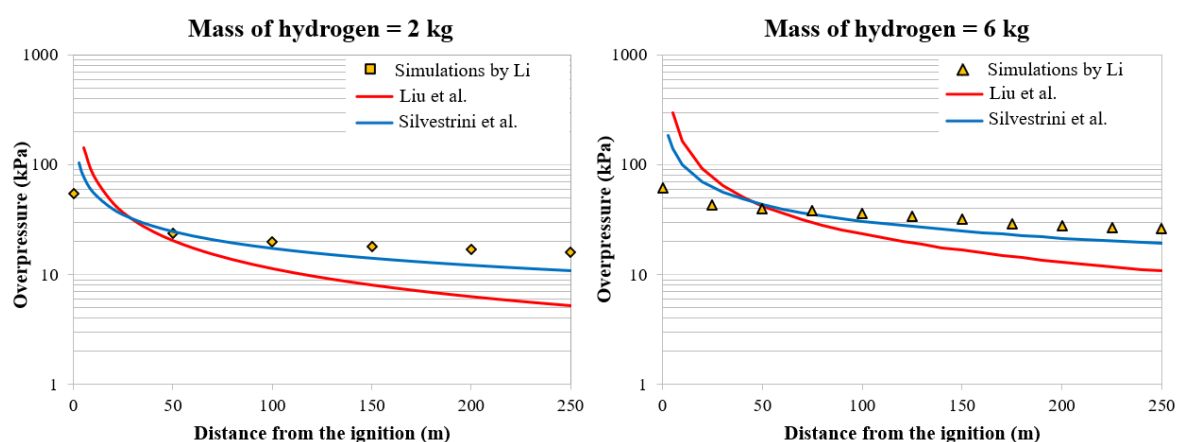
Figure 8. Comparison between the overpressure over distance from the ignition point estimated using the aforementioned simplified methods and that obtained from CFD simulations by Li [36] in the event of deflagration involving: (a) 2 kg; (b) 6 kg of hydrogen.

4.2.2 Overpressures estimated by the simplified method.

As aforementioned, the minimum energy needed for the ignition of the flammable cloud is when the hydrogen concentration is at a stoichiometric ratio with air (i.e., 29.5%). Therefore, we assumed that the ignition occurred in the vicinity of the release location where the presence of hydrogen at stoichiometric concentration is greater, as can be seen from the chromatic scale in the previous Figure 7. A similar location (i.e., within 1 m distance of the release source) was also considered in the study by Venetsanos et al. [14]. With reference to the ignition time, instead, there is no single shared reference in the literature since the flammable cloud might be ignited at any time after the leakage. The ignition time was then assumed in this study as the time at which the most unfavorable conditions for the people evacuation process are present [48]. Specifically, the worst condition for users was

found when the ignition of the hydrogen-air mixture occurs 90 s after the start of the release (see the following Figure 9). Finally, to estimate the overpressure, only the hydrogen mass at the stoichiometric concentration in air – which was then converted into Trinitrotoluene (TNT) equivalent mass in order to apply the simplified method by Silvestrini et al. [47] – was considered to be involved in the deflagration [17]. Specifically, the following relationship was used to convert the hydrogen mass into the corresponding TNT equivalent mass [47]:

$$m_{TNT} = \alpha \frac{m_{H2} \cdot H_{H2}}{H_{TNT}}, \tag{2}$$

where m_{TNT} – equivalent mass of TNT, kg; α – equivalency factor; m_{H2} – mass of hydrogen, kg; H_{H2} – heat of combustion of hydrogen, J/kg; H_{TNT} – heat of combustion of TNT, J/kg. For example, given that H_{H2} is $141.8 \cdot 10^6$ J/kg, H_{TNT} is $4.42 \cdot 10^6$ J/kg, α is 0.1 for very reactive gases released in confined spaces [47], and m_{H2} is 54 kg after 90 s from the start of LH$_2$ release, the equivalent mass of TNT was computed to be equal to 173 kg.

Figure 9 shows the overpressures over distance as a consequence of the hydrogen deflagration within the investigated tunnel tube for different ignition times when the leakage occurs in the middle of the tunnel length. The aforementioned LH$_2$ release location was found to be the worst one in terms of dimensions of the stoichiometric gas cloud because less affected by the presence of the entrance or exit portal where fresh air is present. From Figure 9, it can also be noted the position occupied by the last user escaping from the tunnel tube towards the entrance portal at different times after the release. Considering a pre-movement time of 90 s and a walking speed of 0.5 m/s, the mentioned user is 479, 429, 379, 329, 279, and 229 m from the entrance portal after 100, 200, 300, 400, 500, and 600 s from the start of release, respectively. In particular, the worst condition in terms of maximum overpressure experienced by the user was found when the ignition of the hydrogen-air mixture occurred 90 s after the start of release (i.e., at the end of the pre-movement time). At that moment, the user is still at his/her initial position (i.e., 484 m from the entrance portal of the tunnel) and the maximum overpressure was computed to be about 220 kPa. For ignition times less than 90 s, the mass of hydrogen contained within the cloud is too small (e.g., after 50 s from the release the hydrogen mass was about 29 kg leading to a maximum overpressure of 160 kPa); while for ignition times higher than 90 s, although the mass of hydrogen increased and so did the overpressures, the user is at a distance from the ignition location such that the maximum overpressure is lower than that related to the ignition time of 90 s. It is to be mentioned that the other investigated locations of the release (not reported here) led to similar results.
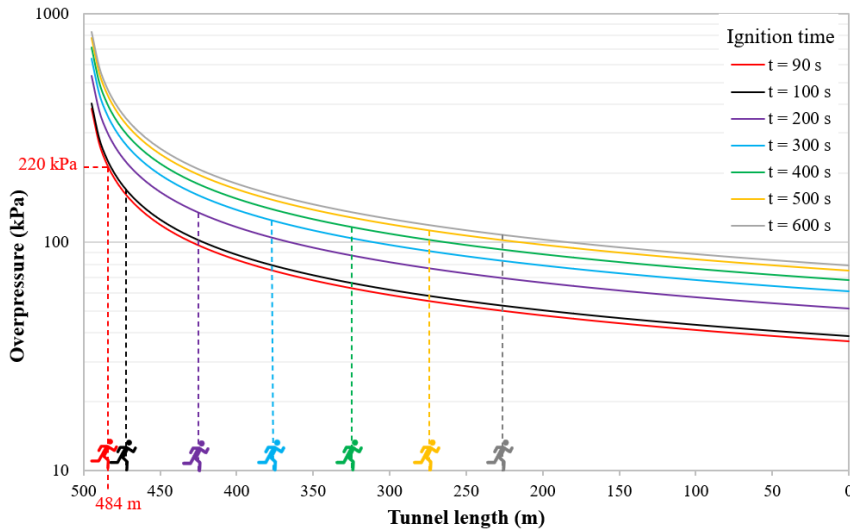
Figure 9. Overpressures over distance as a consequence of the hydrogen deflagration within the investigated tunnel for different ignition times when the release is in the middle of the tunnel length.

4.3 User safety

On the basis of the overpressures generated from the hydrogen deflagration within the investigated

tunnel, an effect model inform of a probit function was used to predict the level of harm to people while escaping towards a safe place (i.e., the entrance portal of the tunnel tube in this case). Probit functions, which are widely used for risk assessment, translate the harm level to a probability of injury and/or fatality. In this respect, several probit functions for damage caused by overpressure hazards are available in the literature but, with reference to human fatality, the Eisenberg model [49] was used in the present paper because it was found to fit better with literature data [50]. Specifically, the aforementioned model is based on an analytical equation that correlates a given overpressure value with the probability of human fatality due to lung hemorrhage. Then, by knowing the position of each user within the tunnel tube during the evacuation process it is possible to estimate the number of people exposed to a given overpressure and their probability of fatality. Moreover, in order to consider also the case in which the first vehicle in the queue upstream of the LH_2 road tanker might be a bus, a pre-movement time of 150 s (i.e., increased by 60 s when compared to the pre-movement time of a passenger car to take into account the time required by users to get off the bus [51]) was subsequently investigated in the present paper. Figure 10 shows the number of potential fatalities due to lung hemorrhage caused by overpressures for a users' pre-movement time of 90 and 150 s, respectively.
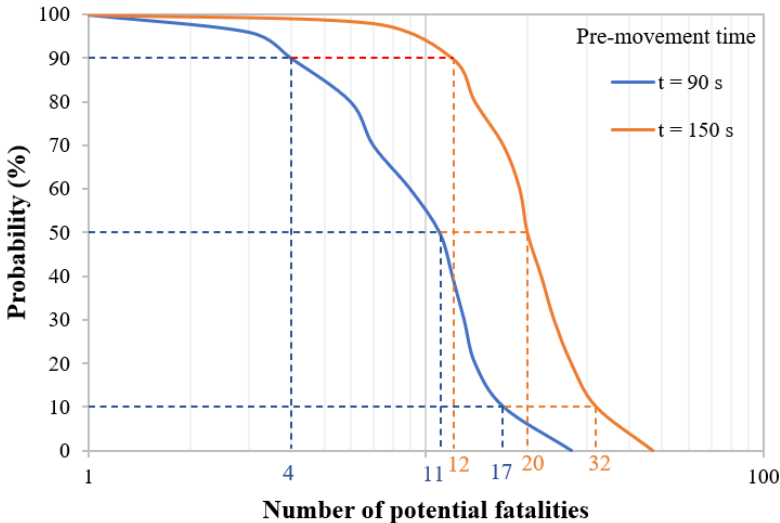
Figure 10. Number of potential fatalities due to lung hemorrhage caused by overpressures when the release is in the middle of the tunnel length.

From Figure 10, it can be noted that the number of potential fatalities significantly increased as the pre-movement time increased (i.e., passing from 90 s to 150 s). Specifically, with reference to a 90% probability of death, the number of potential fatalities within the investigated tunnel tube increased from 4 to 12 passing from a pre-movement time of 90 s to 150 s, respectively. Similarly, a 50% probability of death is associated with 11 and 17 potential victims. Likewise, for a given number of potential victims, the probability of death significantly increases with the pre-movement time. Therefore, the people evacuation process should start as soon as possible when an accidental release of LH_2 occurs in a road tunnel.

5.0 CONCLUSIONS

A 3D Computational Fluid Dynamics (CFD) model for the release of liquid hydrogen (LH_2) from a tanker and its dispersion within a 1 km-long road tunnel was developed and validated in this study. The results of the simulations of the hydrogen dispersion within the investigated tunnel were combined with an established simplified method available in the literature to estimate the overpressure generated from a potential deflagration. Based on the overpressures, a probit function was used to predict the level of harm to users while escaping towards a safe place. Therefore, the number of people exposed to the risk of death due to lung hemorrhage, as well as its probability, was estimated. The findings showed that the worst scenario is when the release is in the middle of the tunnel length and the ignition occurs 90 s after the leakage. The assumption that the first vehicle in the queue might be a bus was also considered in the study, which was done by imposing a higher pre-movement time of users due to the increased time required by all the passengers to get off the bus. The number of

potential fatalities, under the same probability of death, was found to significantly increase as the pre-movement time increased (i.e., passing from 90 s to 150 s). Or in other terms, for a given number of potential victims, the probability of death significantly increases with the pre-movement time. This means that the evacuation process should start as soon as possible when an accidental release of LH$_2$ occurs in a road tunnel. Although this study might represent an advancement of research, there are still some points that need to be investigated. More especially, a specific CFD model to estimate the overpressures due to hydrogen deflagration should be developed. Moreover, different geometries and lengths of the tunnels and/or bi-directional traffic flow conditions, as well as specific mitigation measures to reduce the risk due to the release of hydrogen, should also be investigated.

REFERENCES

[1] European Commission, The European Green Deal, Brussels, 11 December 2019.

[2] Caliendo, C., Russo, P. and Ciambelli, P., Hydrogen safety, state of the art, perspectives, risk assessment, and engineering solutions, Volume 3 Utilization of Hydrogen for Sustainable Energy and Fuels, De Gruyter, Berlin, 2021, pp. 433–449.

[3] Markert, F., Nielsen, S.K., Paulsen, J.L., Andersen, V., Safety aspects of future infrastructure scenarios with hydrogen refuelling stations, *International Journal of Hydrogen Energy*, **32**, No. 13, 2227, 2234.

[4] Mahajan, D., Tan, K., Venkatesh, T., Kileti, P. and Clayton, C.R., Hydrogen Blending in Gas Pipeline Networks—A Review, *Energies*, **15**, No. 10, 2022, 3582.

[5] Ball, M. and Wietschel, M., The future of hydrogen - opportunities and challenges, *International Journal of Hydrogen Energy*, **34**, No. 2, 2009, pp. 615–627.

[6] Hall, J., Ignited releases of liquid hydrogen, RR987 Research Report, Health and Safety Laboratory, 2014.

[7] Dagdougui, H., Sacile, R., Bersani, C. and Ouammi, A., Hydrogen Storage and Distribution: Implementation Scenarios, Hydrogen Infrastructure for Energy Applications, Academic Press, 2018, pp. 37–52.

[8] Jordan, T., Jallais, S., Bernard, L., Venetsanos, A., Coldrick, S., Kuznetsov, M. and Cirrone, D., Status of the pre-normative research project PRESLHY for the safe use of liquid hydrogen, Proceedings of the International Conference on Hydrogen Safety, 24-26 September 2019.

[9] Xu, B., Jallais, S., Houssin, D., Vyazmina, E., Bernard, L. and Wen, J.X., Numerical simulations of atmospheric dispersion of large-scale liquid hydrogen releases, Proceeding of the International Conference on Hydrogen Safety, 21-23 September 2021.

[10] He, P., Li, X., Bénard, P., Chahine, R. and Xiao, J., CFD model based ANN prediction of flammable vapor cloud formed by liquid hydrogen spill, Proceedings of the International Conference on Hydrogen safety, 21-23 September 2021.

[11] Bernard, L., Houssin, D., Jallais, S., Jordan, T. and Cirrone, D., Novel guidelines for safe design and operation of LH$_2$ systems and infrastructure, Pre-normative REsearch for Safe use of Liquid Hydrogen (PRESLHY), Deliverable Number: D6.2, Work Package: WP6, 2021.

[12] Kožuh, M., Preventing hydrogen detonations in road tunnels hydrogen trap concept, *International Journal of Hydrogen Energy*, **39**, No. 30, 2014, pp. 17434–17439.

[13] Utgikar, V.P. and Thiesen, T., Safety of compressed hydrogen fuel tanks: Leakage from stationary vehicles, *Technology in Society*, **27**, No. 3, 2005, pp. 315–320.

[14] Venetsanos, A.G., Baraldi, D., Adams, P., Heggem, P.S. and Wilkening, H., CFD modelling of hydrogen release, dispersion and combustion for automotive scenarios, *Journal of Loss Prevention in the Process Industries*, **21**, No. 2, 2008, pp. 162–184.

[15] Statharas, J.C., Venetsanos, A.G., Bartzis, J.G., Würtz, J. and Schmidtchen, U., Analysis of data from spilling experiments performed with liquid hydrogen, *Journal of Hazardous Material*, **77**, No. 1, 2000, pp. 57–75.

[16] Sklavounos, S. and Rigas, F., Fuel gas dispersion under cryogenic release conditions, *Energy & Fuels*, **19**, No. 6, 2005, pp. 2535–2544.

[17] Middha, P. and Hansen, O.R., CFD simulation study to investigate the risk from hydrogen vehicles in tunnels, *International Journal of Hydrogen Energy*, **34**, No. 14, 2009, pp. 5875–5886.

[18] Unno, S., Takaoka, Y., Kamiya, S., Oyama, S., Kishimoto, A., Miida, A. and Suga, H., A study on dispersion resulting from liquefied hydrogen spilling, Proceedings of the International Conference on Hydrogen Safety, 19-21 October 2015.

[19] Jin, T., Wu, M., Liu, Y., Lei, G., Chen, H. and Lan, Y., CFD modeling and analysis of the influence factors of liquid hydrogen spills in open environment, *International Journal of Hydrogen Energy*, **42**, No. 1, 2017, pp. 732–739.

[20] Liu, Y., Wei, J., Lei, G., Lan, Y., Chen, H. and Jin, T., Dilution of hazardous vapor cloud in liquid hydrogen spill process under different source conditions, *International Journal of Hydrogen Energy*, **43**, No. 15, 2018, pp. 7643–7651.

[21] Giannissi, S.G. and Venetsanos, A.G., A comparative CFD assessment study of cryogenic hydrogen and LNG dispersion, *International Journal of Hydrogen Energy*, **44**, 2019, pp. 9018–9030.

[22] Liu Y., Wei, J., Lei, G., Chen, H., Lan, Y., Gao, X., Wang, T. and Jin, T., Spread of hydrogen vapor cloud during continuous liquid hydrogen spills, *Cryogenics*, **103**, 2019, 102975.

[23] Pu, L., Shao, X., Zhang, S., Lei, G. and Li, Y., Plume dispersion behaviour and hazard identification for large quantities of liquid hydrogen leakage, *Asia-Pacific Journal of Chemical Engineering*, **14**, No. 2, 2019, e2299.

[24] Hansen, O.R., Liquid hydrogen releases show dense gas behavior, *International Journal of Hydrogen Energy*, **45**, No. 2, 2020, pp. 1343–1358.

[25] Tang, X., Pu, L., Shao, X., Lei, G., Li, Y. and Wang, X., Dispersion behavior and safety study of liquid hydrogen leakage under different application situations, *International Journal of Hydrogen Energy*, **45**, No. 55, 2020, pp. 31278–31288.

[26] Ustolin, F. and Paltrinieri, N., Hydrogen fireball consequence analysis, *Chemical Engineering Transactions*, **82**, 2020, pp. 211–216.

[27] Caliendo, C. and Genovese, G., Quantitative Risk Assessment on the Transport of Dangerous Goods Vehicles Through Unidirectional Road Tunnels: An Evaluation of the Risk of Transporting Hydrogen, *Risk Analysis*, **41**, No. 9, 2021, pp. 1522–1539.

[28] Liu, Y., Liu, Z., Wei, J., Lan, Y., Yang, S. and Jin, T. Evaluation and prediction of the safe distance in liquid hydrogen spill accident, *Process Safety and Environmental Protection*, **146**, 2021, pp. 1–8.

[29] Cirrone, D., Makarov, D., Molkov, V., Venetsanos, A., Coldrick, S., Atkinson, G., Proust, C., Friedrich, A. and Kuznetsov, M., Detailed description of novel engineering correlations and tools for LH2 safety, version 2, Pre-normative REsearch for Safe use of Liquid Hydrogen (PRESLHY), Deliverable Number: D6.5, Work Package: WP6, 2021.

[30] Directive 2004/54/EC, European Parliament and Council, Official Journal of the European Union, 2004.

[31] Ciambelli, P., Meo, M.G., Russo, P. and Vaccaro, S., Natural Vs Forced Ventilation During Fires In Relatively Short Road Tunnels, Proceedings of 29th Meeting of the Italian Section of the Combustion Institute, Pisa, Italy, 14-17 January 2006.

[32] Schrefler, B.A., Brunello, P., Gawin, D., Majorana, C.E. and Pesavento, F. Concrete at high temperature with application to tunnel fire, *Computational Mechanics*, **29**, No. 1, 2002, pp. 43–51.

[33] Bonati, A., Rainieri, S., Bochicchio, G., Tessardi, B. and Giuliani, F., Characterization of thermal properties and combustion behaviour of asphalt mixtures in the cone calorimeter, *Fire Safety Journal*, **74**, 2015, pp. 25–31.

[34] Caliendo, C., Genovese, G. and Russo, I., Risk Analysis of Road Tunnels: A Computational Fluid Dynamic Model for Assessing the Effects of Natural Ventilation, *Applied Sciences*, **11**, 2021, 32.

[35] Hall, J.E., Hooker, P. and Willoughby, D., Ignited releases of liquid hydrogen: Safety considerations of thermal and overpressure effects, *International Journal of Hydrogen Energy*, **39**, No. 35, 2014, pp. 20547–20553.

[36] Li, Y.Z., Fire and explosion hazards of alternative fuel vehicles in tunnels, Research Institutes of Sweden, Rapport 2018:20, 2018.

[37] Bahuguni, A., Kumara, A.S. and Giljarhus, K.E.T., Modelling of hydrocarbon gas and liquid leaks from pressurized process systems, *International Journal of Computational Methods and Experimental Measurements*, **7**, No. 2, 2019, pp. 154–166.

[38] Caliendo, C., Ciambelli, P., De Guglielmo, M.L., Meo, M.G. and Russo, P., Computational analysis of fire and people evacuation for different positions of burning vehicles in a road tunnel with emergency exits, *Cogent Engineering*, **5**, No. 1, 2018, 1530834.

[39] Ansys Inc., Ansys Fluent User's Guide, 2022 R1.

[40] Shao, X., Pu, L., Li, Q. and Li, Y. Numerical investigation of flammable cloud on liquid hydrogen spill under various weather conditions, *International Journal of Hydrogen Energy*, **43**, No. 10, 2018, pp. 5249–5260.

[41] Sun, R., Pu, L., Yu, H., Dai, M. and Li, Y., Investigation of the hazardous area in a liquid hydrogen release with or without fence, *International Journal of Hydrogen Energy*, **46**, No. 73, 2021, pp. 36598–36609.

[42] Verfondern, K. and Teodorczyk, A., Hydrogen Fundamentals, Biennal Report on Hydrogen Safety, 2007.

[43] Xie, Y., Lv, N., Wang, X., Wu, D. and Wang, S., Thermal and fire characteristics of hydrogen jet flames in the tunnel at longitudinal ventilation strategies, *Fuel*, **306**, 2021, 121659.

[44] Witcofski, R.D. and Chirivella, J.E., Experimental and analytical analyses of the mechanisms governing the dispersion of flammable clouds formed by liquid hydrogen spills, *International Journal of Hydrogen Energy*, **9**, No. 5, 1984, pp. 425–435.

[45] Molkov, V. and Dery, W., The blast wave decay correlation for hydrogen tank rupture in a tunnel fire, *International Journal of Hydrogen Energy*, **45**, No. 55, 2020, pp. 31289–31302.

[46] Liu, J., Yan, Q. and Wu, J., Analysis of blast wave propagation inside tunnel, *Transactions of Tianjin University*, **14**, No. 5, 2008, pp. 358–362.

[47] Silvestrini, M., Genova, B. and Trujillo, F.J.L., Energy concentration factor. A simple concept for the prediction of blast propagation in partially confined geometries, *Journal of Loss Prevention Process in the Process Industries*, **22**, No. 4, 2009, pp. 449–454.

[48] Li, Y., Xiao, J., Zhang, H., Breitung, W., Travis, J., Kuznetsov, M. and Jordan, T., Numerical analysis of hydrogen release, dispersion and combustion in a tunnel with fuel cell vehicles using all-speed CFD code GASFLOW-MPI, *International Journal of Hydrogen Energy*, 46, No. 23, 2021, pp. 12474–12486.

[49] Center for Chemical Process Safety of the American Institute of Chemical Engineers. Guidelines for Chemical Process Quantitative Risk Analysis, Second Edition, 1999, John Wiley & Sons, Inc., Publication, New York.

[50] LaChance, J., Tchouvelev, A. and Engebo, A., Development of uniform harm criteria for use in quantitative risk analysis of the hydrogen infrastructure, *International Journal of Hydrogen Energy*, **36**, No. 3, 2011, pp. 2381–2388.

[51] Xie, B., Zhang, S., Xu, Z., He, L., Xi, B. and Wang, M. Experimental study on vertical evacuation capacity of evacuation slide in road shield tunnel, *Tunnelling and Underground Space Technology*, **97**, 2020, 103250.